



# Edge states in a ferromagnetic honeycomb lattice with armchair boundaries

Pierre A. Pantaleón<sup>\*</sup>, Y. Xian

Theoretical Physics Division, School of Physics and Astronomy, University of Manchester, Manchester M13 9PL, United Kingdom



## ARTICLE INFO

### Keywords:

Bosonic edge states  
Magnon topological insulators  
Magnonics  
Honeycomb ferromagnetic lattice

## ABSTRACT

We investigate the properties of magnon edge states in a ferromagnetic honeycomb lattice with armchair boundaries. In contrast with fermionic graphene, we find novel edge states due to the missing bonds along the boundary sites. After introducing an external on-site potential at the outermost sites we find that the energy spectra of the edge states are tunable. Additionally, when a non-trivial gap is induced, we find that some of the edge states are topologically protected and also tunable. Our results may explain the origin of the novel edge states recently observed in photonic lattices. We also discuss the behavior of these edge states for further experimental confirmations.

## 1. Introduction

One intriguing aspect of electrons moving in finite-sized honeycomb lattices is the presence of edge states, which have strong implications in the electronic properties and play an essential role in the electronic transport [1–3]. It is well known that natural graphene exhibits edge states under some particular boundaries [4,5]. For example, there are flat edge states connecting the two Dirac points in a lattice with zig-zag [1] or bearded edges [6]. On the contrary, there are no edge states in a lattice with armchair boundary [7], unless a boundary potential is applied [8].

The edge states have also been studied in magnetic insulators [9–11], where the spin moments are carried by magnons. Recently, it has been shown that the magnonic equivalence for the Kane-Mele-Haldane model is a ferromagnetic Heisenberg Hamiltonian with the Dzialozinskii-Moriya interaction [12,13]. Firstly, while the energy band structure of the magnons of ferromagnets on the honeycomb lattice closely resembles that of the fermionic graphene [14,15], it is not clear whether or not they show similar edge states, particularly in view of the interaction terms in the bosonic models which are usually ignored in graphene [16]. Secondly, most recent experiments in photonic lattices have observed novel edge states in honeycomb lattices with bearded [17] and armchair [18] boundaries, which are not present in fermionic graphene. The main purpose of this paper is to address these two issues. By considering a ferromagnetic honeycomb lattice with armchair boundaries, we find that the bosonic nature of the Hamiltonian reveals novel edge states which are not present in their fermionic counterpart. After introducing an external on-site potential at the outermost

sites, we find that the edge states are tunable. Interestingly, we find that the nature of such edge states is Tamm-like [19], in contrast with the equivalent model for armchair graphene [8] but, as mentioned earlier, in agreement with the experiments in photonic lattices [17,18]. Furthermore, after introducing a Dzialozinskii-Moriya interaction (DMI), we find that the topologically protected edge states are sensitive to the presence of the Tamm-like states and they also become tunable.

## 2. Model Hamiltonian

We consider the following Hamiltonian for a ferromagnetic honeycomb lattice,

$$H = -J \sum_{\langle i,j \rangle} S_i \cdot S_j + \sum_{\langle\langle i,j \rangle\rangle} D_{ij} \cdot (S_i \times S_j), \quad (1)$$

where the first summation runs over the nearest-neighbors (NN) and the second over the next-nearest-neighbors (NNN),  $J > 0$  is the isotropic ferromagnetic coupling,  $S_i$  is the spin moment at site  $i$  and  $D_{ij}$  is the DMI vector between NNN sites [20]. If we assume a lattice in the  $x$ - $y$  plane, according to Moriya's rules [20], the DMI vector vanishes for the NN but has non-zero component along the  $z$  direction for the NNN. Hence, we can assume  $D_{ij} = D v_{ij} \hat{z}$ , where  $v_{ij} = \pm 1$  is an orientation dependent coefficient in analogy with the Kane-Mele model [21]. For the infinite system in the linear spin-wave approximation (LSWA), the Hamiltonian in Eq. (1) can be reduced to a bosonic equivalent of the Kane-Mele-Haldane model [12–14]. To investigate the edge states we consider an armchair boundary along the  $x$  direction, with a large  $N$  sites in the  $y$  direction, as shown in Fig. (1). A partial Fourier transform is made and

<sup>\*</sup> Corresponding author.

E-mail address: [ppantaleon@uabc.edu.mx](mailto:ppantaleon@uabc.edu.mx) (Pierre A. Pantaleón).

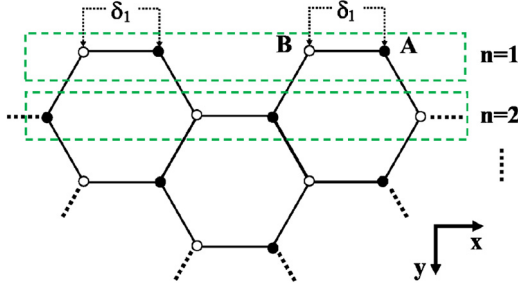


Fig. 1. Schematics of the upper armchair edge of a honeycomb lattice. The external on-site potential  $\delta_1$  is applied at the outermost sites. Here,  $n$  is a real-space row index in  $y$  direction perpendicular to the edge. For a large  $N$ , we consider the opposite edge with the same structure and with an on-site potential  $\delta_N$ .

the Hamiltonian given in Eq. (1) in LSWA can be written in the form,

$$H = -t \sum_k \Psi_k^\dagger M \Psi_k, \quad (2)$$

where  $\Psi_k^\dagger = [\Psi_{k,A}^\dagger, \Psi_{k,B}^\dagger]$  is a  $2N \times 2N$ , 2-component spinor,  $k$  is the Bloch wave number in the  $x$  direction and  $t = JS$ . The matrix elements of  $M$  are  $N \times N$  matrices given by,

$$\begin{aligned} M_{11} &= (1 - \delta_1) T^\dagger T + (1 - \delta_N) T T^\dagger + \delta_s I + M_D, \\ M_{12} &= -J_1 I - J_2 (T + T^\dagger), \\ M_{21} &= M_{12}^\dagger, \\ M_{22} &= M_{11} - 2M_D, \end{aligned} \quad (3)$$

with  $\delta_s = (1 + \delta_1 + \delta_N) I$  and  $M_D = J_3 (T T^\dagger - T^\dagger T) + J_4 (T^\dagger - T)$  the DMI contribution. Here,  $T$  is a displacement matrix as defined in Ref. [22] and  $I$  a  $N \times N$  identity matrix. We have also introduced two on-site energies  $\delta_1$  and  $\delta_N$  at the outermost sites of each boundary, respectively. The coupling terms are:  $J_1 = e^{-ik}$ ,  $J_2 = e^{ik/2}$ ,  $J_3 = iD'$ ,  $J_4 = 2iD' \cos(3k/2)$  and  $D' = D/J$ . The numerical diagonalization of the matrix given by Eq. (2) reveals that the bulk spectra is gapless only if  $N = 3m + 1$ , with  $m$  a positive integer [23]. However, to avoid size-dependent bulk gaps or hybridization between edge states of opposite edges [8], we consider a large  $N$  where the edge states are independent of the size [24,25].

### 3. Edge states and boundary conditions

From the explicit form of the matrix elements given in Eq. (3), the coupled Harper equations can be obtained [26]. If we assume that the edge states are exponentially decaying from the armchair boundary, we can consider the following ansatz [27,28] for the eigenstates of  $M$  in Eq. (2),

$$\Psi_k(n) = \begin{bmatrix} \psi_{k,A}(n) \\ \psi_{k,B}(n) \end{bmatrix} = z^n \begin{bmatrix} \phi_{k,A} \\ \phi_{k,B} \end{bmatrix}, \quad (4)$$

where  $[\phi_{k,A}, \phi_{k,B}]^t$  is an eigenvector of  $M$ ,  $z$  is a complex number and  $n\{= 1, 2, 3, \dots\}$  is a real space lattice index in the  $y$  direction, as shown in Fig. (1). Upon substitution of the ansatz in the coupled Harper equations, the complex number  $z$  obey the following polynomial equation,

$$\sum_{\mu=0}^4 a_\mu (z + z^{-1})^\mu = 0, \quad (5)$$

with coefficients:  $a_0 = 1 - (3 - \varepsilon)^2 - 4J_4^2$ ,  $a_1 = 8J_3J_4 + J_1^*J_2 + J_2^*J_1$ ,  $a_2 = -4J_3^2 + J_4^2 + 1$ ,  $a_3 = -2J_3J_4$  and  $a_4 = J_3^2$ . For a given  $k$  and energy  $\varepsilon$ , such a polynomial always yields four solutions for  $(z + z^{-1})$ . Since we require a decaying wave from the boundary, only the solutions with  $|z| < 1$

are relevant for the description of the edge states at the upper edge and  $|z| > 1$  for the lower (opposite) edge. The eigenfunction of Eq. (2) satisfying  $\lim_{n \rightarrow \infty} \Psi_k(n) = 0$  may now in general be written as,

$$\psi_{k,l}(n) = \sum_{v=1}^4 c_v z_v^n \phi_{l,v}, \quad (6)$$

where the coefficients  $c_v$  are determined by the boundary conditions and  $\phi_{l,v}$  is the two-component eigenvector ( $l = A, B$ ) of  $M$ . From the Harper equations provided by the Eq. (3) and Eq. (4), the boundary conditions are satisfied by,

$$(1 - \delta_1) \psi_{k,A}(1) - J_2 \psi_{k,B}(0) = 0, \quad (7)$$

$$(1 - \delta_1) \psi_{k,B}(1) - J_2^* \psi_{k,A}(0) = 0, \quad (8)$$

$$J_4 \psi_{k,A}(0) - J_3 \psi_{k,A}(-1) = 0, \quad (9)$$

$$J_4 \psi_{k,B}(0) - J_3 \psi_{k,B}(-1) = 0. \quad (10)$$

By Eq. (6), the above relations can be written as a set of equations for the unknown coefficients  $c_v$ . The non-trivial solution and the polynomial given by Eq. (5), provide us a complete set of equations for the edge state energy dispersion and they can be solved numerically. The same procedure can be followed to obtain the solutions for the opposite edge.

## 4. Results and discussions

### 4.1. Zero DMI

For the system without DMI, the coupling terms involving  $J_3$  and  $J_4$  vanish, and the boundary conditions are reduced to the Eqs. (7) and (8) with a quadratic polynomial in  $(z + z^{-1})$  of Eq. (5). In particular, for the (uniform) case with  $\delta_1 = \delta_N = 1$ , the edge and the bulk sites have the same on-site potential and the boundary conditions provide us with two bulk solutions with  $z^2 = 1$ . Therefore, in analogy with graphene with armchair edges, there are not edge states [7]. However, as shown in Fig. (2a), in the absence of external on-site potential ( $\delta_1 = \delta_N = 0$ ), two new dispersive localized modes are obtained. Located between (red, continuous line) and below (green, dotted) the bulk bands, such edge states are well defined along the Brillouin zone and their energy bands are doubly degenerated due to the fact that there are two edges in the ribbon. These edge states have not been previously predicted or observed in magnetic insulators. However, we believe that they are analogous to the novel edge states recently observed in a photonic honeycomb lattice with armchair edges [18]. Although in Ref. [18] these edge states may be attributed to the dangling bonds along the boundary sites (the details have been given for zig-zag and bearded but not for armchair edges), and since these dangling bonds can be viewed as effective defects along the edges, similar physics is contained in our model where the effective defects are described by the different on-site potential at the boundaries. We believe that our approach has the advantage of simple implementation for various boundary conditions. In particular, we have obtained expressions for the wavefunctions and their confinement along the boundary. The latter is given by the penetration length (or width) of the edge state [29] defined as,

$$\xi_i(k) \equiv \frac{\sqrt{3}}{2} \left[ \ln \left| \frac{1}{z_i(k)} \right| \right]^{-1}, \quad (11)$$

indicating a decay of the form  $\sim e^{-y/\xi_i(k)}$ . In the above equation,  $z_i$  is the  $i$ -th decaying factor in the linear combination, Eq. (6). Since we require two decaying factors to construct the edge state, we have two penetration lengths as mentioned in Ref. [18]. The penetration lengths for the edge states with  $\delta_1 = \delta_N = 0$  are shown in the Fig. (2b). The

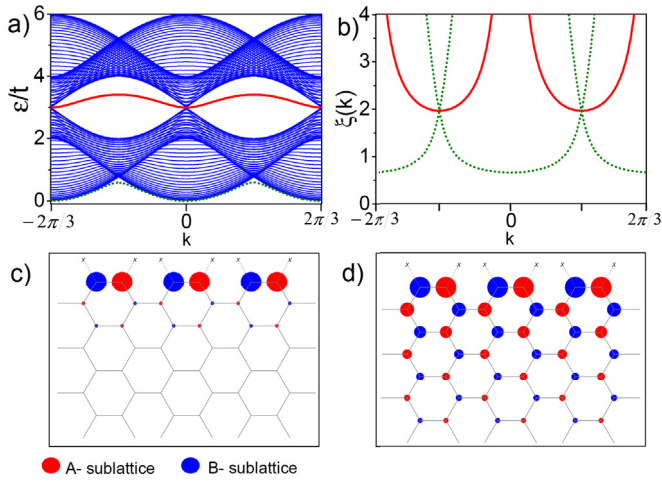


**Fig. 2.** a) Edge state energy dispersion for  $D = 0$  and  $\delta_1 = \delta_N = 0$ . The blue regions are the bulk energy spectra. The green (dotted) and red (continuous) lines are the edge state energy bands. In b) their corresponding penetration lengths are shown. The magnon density profile for the edge magnon is shown in c) for  $\epsilon = (2 \pm \sqrt{2})t$  at  $k = \pm\pi/3$ , and in d) for  $\epsilon = 0.298t$  at  $k = \pm 0.65$ . The radius of each circle is proportional to the magnon density. (For interpretation of the references to colour in this figure legend, the reader is referred to the web version of this article.)

dotted (green) and continuous (red) lines are the corresponding penetration lengths for the edge states in the Fig. (2a). The edge state between the bulk bands (red, continuous) is composed by two penetration lengths but they are indistinguishable to each other. This indicates that the decaying factors are complex conjugates to each other,  $z_1 = z_2^*$  [14,29]. The edge state below the lower bulk band (green, dotted) depends on two penetration lengths in the region around  $k = \pm\pi/3$ . However, outside such region, one penetration length diverges, that is  $|z| \rightarrow 1$ , while the other one decreases to a minimum value. This means that the edge state tends to merge with the bulk and is almost indistinguishable at  $k = 0, \pm 2\pi/3$ . Furthermore, as we can see in the Fig. (2b), at  $k = \pm\pi/3$ , the penetration length of both edge states is identical hence they have their maximum confinement along the boundary at the same Bloch wave-vector. This is shown in the Fig. (2c) where we plot the magnon density,  $|\psi_{k,l}(n)/\psi_{k,l}(1)|^2$ , for both edge states at  $k = \pm\pi/3$  with their corresponding energies,  $\epsilon = (2 \pm \sqrt{2})t$ . In addition, in the Fig. (2d) the magnon density for the edge state below the lower bulk band with energy  $\epsilon = 0.298t$  at  $k = \pm 0.65$  is shown, where as we mentioned before, if  $k$  approaches to zero, the edge state tends to spread to the inner sites.

The edge states described before have been obtained with no gap in the bulk for a non-interacting bosonic Hamiltonian, Eq. (2) and for  $\delta_1 = \delta_N = 0$ . They are located between the Dirac points and their existence without external on-site potentials indicates that they are “Tamm-like” [17,19]. Such type of states are usually associated with surface perturbations or defects. However, in our system no defects are present. The origin of such edge states is related to the on-site contribution along the boundary, where each site has two nearest neighbors hence the on-site potential is lower than in the bulk. Such difference creates an effective defect and induces the “Tamm-Like” edge states. We also like to point that such on-site potentials come from the original spin-model of Eq. (1). In analogy with the photonic model described in Ref. [17], the missing bonds along the boundary give rise to a reduction of the on-site potential and makes the edge itself a defect. This is taken into account in the first terms of both Eq. (7) and Eq. (8), which contains the on-site contribution to the boundary conditions in both sublattices. Such on-site terms are missing in their fermionic counterpart. This may explain why the observed edge states discussed in this paper do not exist in graphene unless an edge potential be applied [8].

We next discuss the effects of edge potentials. It has been shown that edge states can be induced by edge potentials in the armchair graphene [8], however, the edge states that we found are a consequence of the bosonic nature of the lattice as discussed above. Since they exist without opening a gap and they are dispersive, it is not clear if they can be predicted by a topological approach. Our approach reveals that the edge states in a bosonic lattice are strongly dependent on the on-site potential along the boundary. For example, if  $\delta_1 = 2.5$  (with  $\delta_N = 0$ ) some new features are obtained. As shown in Fig. (3a), the presence of the strong external on-site potential reveals three edge states at the upper boundary: a high energy edge state over the bulk bands (black, continuous line), an edge state between the bulk bands (purple, dot-dashed line), and interestingly, an edge state within the bulk bands (orange circle). Such edge state is strongly localized and is highly dispersive, Fig. (3b). It merges into the bulk with a small change in their Bloch wave-number and may be difficult to detect in a magnetic insulator. It is therefore very encouraging that similar edge state was observed in a photonic lattice [18].

#### 4.2. Non-zero DMI

It is well known that a non-zero DMI in a bosonic honeycomb lattice makes the band structure topologically non-trivial and reveals metallic edge states which transverse the gap [12]. However, the edge states that appear, under, within and over the bulk bands in Figs. (2a) and (3a) are distinct to the edge states predicted by topological arguments.

In the Fig. (4) we show the energy bands for a DMI strength of  $D = 0.1J$ , where we keep a fixed  $\delta_N = 1$  and we modified  $\delta_1$ . The continuous (green) line that cross the gap from the lower to the upper bulk bands is the edge state at the lower edge. The dotted (red) lines correspond to the edge states at the upper edge. If we follow the edge state energy spectra at the upper boundary from the Fig. (4a) to the Fig. (4c), we observe that the edge state within the bulk gap change its concavity. The Tamm-like state below the bulk bands, Fig. (4a), merge with the bulk and a new Tamm-like state appears at the top of the upper bulk band, as shown in Fig. (4c). If we keep increasing the value of the external on-site potential the Tamm-like state over the bulk band in Fig. (4c) moves away from the upper bulk band, Fig. (4d). Furthermore, a second Tamm-like state appears with components within the bulk, as shown in Fig. (4d) and (4e). The boundary conditions suggest that the existence of these two tunable edge states is due to the two sites in the unit cell of the armchair boundary and, by symmetry, the same behavior is expected at the opposite edge. These edge states can be made to locate below, within and over the bulk bands. If a non-trivial gap is induced the topologically protected edge states are also tunable.

Finally, similar phenomena is expected for a lattice with zig-zag or bearded boundaries. In both cases there is a single outermost site and Tamm-like edge states may appear due to the missing bond and/or by

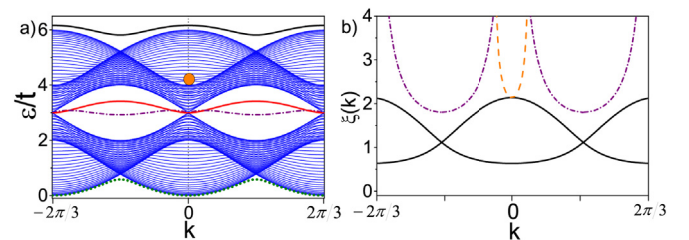


**Fig. 3.** a) Edge state energy dispersion for  $D = 0$  with  $\delta_1 = 2.5$  and  $\delta_N = 0$ . The blue regions are the bulk energy spectra. The dotted (green) and continuous (red) lines are the edge state energy bands at the lower edge. The dot-dashed (purple) line, continuous (black) line and the circle (orange) are the edge states at the upper edge. In b) the penetration lengths of the corresponding edge states at the upper edge is shown. (For interpretation of the references to colour in this figure legend, the reader is referred to the web version of this article.)

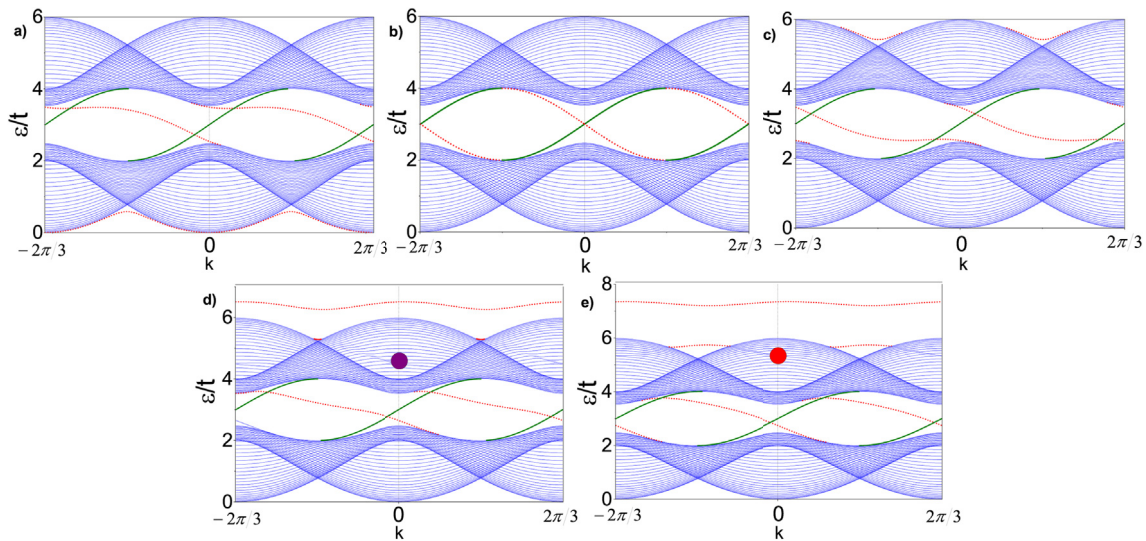


Fig. 4. Edge state energy dispersion for  $D = 0.1J$ . The blue regions are the bulk energy spectra. For  $\delta_N = 1$  (lower edge) there is an edge state crossing the gap (green, continuous). The red (dotted) lines are the edge states for a)  $\delta_1 = 0$ , b)  $\delta_1 = 1$ , c)  $\delta_1 = 2$ , d)  $\delta_1 = 3$  and e)  $\delta_1 = 4$ . The circles in d) and e) are edge states within the bulk energy bands. (For interpretation of the references to colour in this figure legend, the reader is referred to the web version of this article.)

the external on-site potential. Since the outermost site at the lattice with a bearded boundary has three missing bonds, the effective defect should be stronger than the corresponding to a zig-zag boundary. This may be related with the existence of the “unconventional” edge states found in optical lattices [17]. A more extensive investigation of Tamm-like edge states along different boundaries will be reported elsewhere.

## 5. Conclusions

We have analyzed the edge states in a ferromagnetic honeycomb lattice with armchair edges and an external on-site potential at the outermost sites. In contrast with graphene, our system without external on-site potential reveals two edge states. It is clear that the open boundary in a bosonic lattice creates an effective defect by a difference in the on-site potential between the bulk and boundary sites. This effective defect is responsible for the existence of the novel edge states. By introducing an external on-site potential at the outermost sites we found that the nature of this edge states is Tamm-like. We also found that these edge states are tunable in their shapes and positions depending on the external on-site potential strength. Such tunability can be used to modify the topologically protected edge states when a non-trivial gap is induced. Finally, we found that the number of these tunable edge states is related to the number of sites in a unit cell along the boundary. We believe that our results may explain the edge states recently found in optical lattices [17,18] and motivate new experiments in both magnonic and photonic lattices.

## Acknowledgements

Pierre. A. Pantaleón is sponsored by Mexico’s National Council of Science and Technology (CONACYT) under the scholarship 381939.

## References

- [1] M. Fujita, K. Wakabayashi, K. Nakada, K. Kusakabe, *J. Phys. Soc. Jpn.* 65 (1996) 1920.
- [2] K. Nakada, M. Fujita, G. Dresselhaus, M.S. Dresselhaus, *Phys. Rev. B* 54 (1996) 17954.
- [3] M. Kohmoto, Y. Hasegawa, *Phys. Rev. B* 76 (2007) 205402.
- [4] K.W. Akabayashi, S.O. Kada, R.T. Omita, S.F. Ujimoto, Y.N. Atsume, K. Wakabayashi, S. Okada, R. Tomita, S. Fujimoto, Y. Natsume, *J. Phys. Soc. Jpn.* 79 (2010) 034706.
- [5] P. Delplace, D. Ullmo, G. Montambaux, *Phys. Rev. B* 84 (2011) 195452.
- [6] D. Klein, *Chem. Phys. Lett.* 217 (1994) 261.
- [7] Y. Zhao, W. Li, R. Tao, *Phys. B Condens. Matter* 407 (2012) 724.
- [8] C.H. Chiu, C.S. Chu, *Phys. Rev. B* 85 (2012) 155444.
- [9] S. Fujimoto, *Phys. Rev. Lett.* 103 (2009) 047203.
- [10] Y. Onose, T. Ideue, H. Katsura, Y. Shiomi, N. Nagaosa, Y. Tokura, *Science* 329 (2010) 297.
- [11] X. Cao, K. Chen, D. He, *J. Phys. Condens. Matter* 27 (2015) 166003.
- [12] S.A. Owerre, *J. Phys. Condens. Matter* 28 (2016) 386001.
- [13] S.K. Kim, H. Ochoa, R. Zarzuela, Y. Tserkovnyak, *Phys. Rev. Lett.* 117 (2016) 227201.
- [14] P.A. Pantaleón, Y. Xian, *J. Phys. Condens. Matter* 29 (2017) 295701.
- [15] R. Sakaguchi, M. Matsumoto, *J. Phys. Soc. Jpn.* 85 (2016) 104707.
- [16] J. Lado, N. García-Martínez, J. Fernández-Rossier, *Synth. Met.* 210 (2015) 56.
- [17] Y. Plotnik, M.C. Rechtsman, D. Song, M. Heinrich, J.M. Zeuner, S. Nolte, Y. Lumer, N. Malkova, J. Xu, A. Szameit, Z. Chen, M. Segev, *Nat. Mater.* 13 (2014) 57.
- [18] M. Miličević, T. Ozawa, G. Montambaux, I. Carusotto, E. Galopin, A. Lemaître, L. Le Gratiet, I. Sagnes, J. Bloch, A. Amo, *Phys. Rev. Lett.* 118 (2017) 107403.
- [19] I. Tamm, *Phys. Z. Sov. Union* 1 (1923) 733.
- [20] T. Moriya, *Phys. Rev.* 120 (1960) 91.
- [21] C.L. Kane, E.J. Mele, *Phys. Rev. Lett.* 95 (2005) 226801.
- [22] J.S. You, W.M. Huang, H.H. Lin, *Phys. Rev. B* 78 (2008) 161404.
- [23] W.X. Wang, M. Zhou, X. Li, S. Li, X. Wu, W. Duan, L. He, *Phys. Rev. B* 93 (2016) 241403.
- [24] Y. Hatsugai, *Phys. Rev. B* 48 (1993) 11851.
- [25] Y. Hatsugai, *Phys. Rev. Lett.* 71 (1993) 3697.
- [26] P.G. Harper, *Proc. Phys. Soc. Sect. A* 68 (1955) 874.
- [27] M. König, H. Buhmann, L.W. Molenkamp, T. Hughes, C.X. Liu, X.L. Qi, S.C. Zhang, *J. Phys. Soc. Jpn.* 77 (2008) 031007.
- [28] Z. Wang, N. Hao, P. Zhang, *Phys. Rev. B* 80 (2009) 115420.
- [29] H. Doh, G.S. Jeon, *Phys. Rev. B* 88 (2013) 245115.